

These bond numbers indicate a substantial amount of resonance in the ring system. Weakening of the C—C bonds in the benzene ring by this resonance was found in benzotrifuroxan just as it was in 1,3,5-triamino-2,4,6-trinitrobenzene (Cady & Larson, 1965).

We are indebted to Janice Dinegar for her assistance in collecting the intensity data, and to R. B. Roof for his interest and suggestions during the determination of the structure.

References

- BRITTON, D. & NOLAND, W. E. (1962). *J. Org. Chem.* **27**, 3218.
- BUERGER, M. J. (1959). *Vector Space and Its Application in Crystal-Structure Investigation*. New York: John Wiley.
- BUSING, W. R. & LEVY, H. A. (1964). *Acta Cryst.* **17**, 142.
- CADY, H. H. & LARSON, A. C. (1965). *Acta Cryst.* **18**, 485.
- CRUICKSHANK, D. W. J. (1949). *Acta Cryst.* **2**, 65.
- CRUICKSHANK, D. W. J. (1956a). *Acta Cryst.* **9**, 754.
- CRUICKSHANK, D. W. J. (1956b). *Acta Cryst.* **9**, 757.
- CRUICKSHANK, D. W. J. (1961). *Acta Cryst.* **14**, 896.
- EVANS, H. T. (1961). *Acta Cryst.* **14**, 689.
- GOL'DER, G. A., TODRES-SELEKTOR, Z. V. & BOGDANOV, S. V. (1961). *Zh. Strukt. Khim.* **2**, 478.
- HAMILTON, W. C. (1959). *Acta Cryst.* **12**, 609.
- HARRIS, R. K., KATRITZKY, A. R., ØKSNE, S., BAILEY, A. S. & PATTERSON, W. G. (1963). *J. Chem. Soc.* p. 197.
- HOWELLS, E. R., PHILLIPS, D. C. & ROGERS, D. (1950). *Acta Cryst.* **3**, 210.
- HULME, R. (1962). *Chem. and Ind. (London)*, No. 1, 42.
- International Tables for X-Ray Crystallography* (1962). Vol. III, p. 202. Birmingham: Kynoch Press.
- KAUFMAN, J. V. R. & PICKARD, J. P. (1959). *Chem. Rev.* **59**, 429.
- LARSON, A. C., CROMER, D. T. & ROOF, R. B., JR. (1964). Los Alamos Scientific Laboratory Report LA-3043.
- PAULING, L. (1960). *The Nature of the Chemical Bond*. 3rd ed., Chapter 7. Ithaca: Cornell Univ. Press.
- RAMACHANDRAN, G. N. & SRINIVASAN, R. (1959). *Acta Cryst.* **12**, 410.
- TRUEBLOOD, K. N. (1963). Private communication.
- TUREK, O. (1931). *Chim. et Ind.* **26**, 781.
- ZACHARIASEN, W. H. (1963). *Acta Cryst.* **16**, 1139.

Acta Cryst. (1966). **20**, 341

The Structure of Fibrous Sulphur

BY F. TUINSTR

Laboratorium voor Technische Natuurkunde, Technische Rijkshogeschool, Delft, The Netherlands

(Received 21 December 1964 and in revised form 8 March 1965)

The structure of fibrous sulphur has been determined by a systematic use of the Fourier transform of its helical molecules. From this analysis, the helical molecules appeared to have two *incommensurable* repetition lengths in the direction of the helical axis, one being due to the succession of the atoms in that direction, the other to the pitch of the helix. A trial to substitute the two repetition lengths by a single one would result in an infinite repetition length. For this reason the structure is not crystallographic in the classical sense of the word, so we have chosen an improper 'unit cell' of orthorhombic symmetry, containing four helical molecules of supposedly infinite length, with the dimensions $a=8.11 \text{ \AA}$ and $b=9.20 \text{ \AA}$, c =indeterminate. The directions of a and b are normal to the helical axis, but only b is properly a repetition length.

In the direction of a the structure consists of alternating layers of right and left handed helices. Within each layer the helical molecules are screwed in or out, with respect to their neighbours, over half the atomic period along the molecule. This explains a peculiar extinction rule.

The molecular parameters, *i.e.* the bond distance, the bond angle and the dihedral angle, are compared with those of other sulphur molecules.

Introduction

Several physical properties of liquid sulphur suggest that above 160°C it contains long chain molecules (see *e.g.* Schenk, 1956). One of the strongest arguments is provided by the X-ray fibre diagram, obtained from fibres made by highly stretching amorphous sulphur quenched from above 300°C . This diffraction pattern was discovered by Trillat & Forestier (1932); after being wrongly interpreted initially by Meyer & Go (1934) as a one-component pattern, it was later proved (Prins, Schenk

& Hospel, 1956) to be due to two components of which only one is soluble in carbon disulphide. The reflexions due to the soluble part were shown (Prins, Schenk & Wachters, 1957) to belong to a metastable ring modification S_η (De Haan, 1958). The reflexions of the carbon-disulphide-insoluble part evidently formed a fibre diagram. The corresponding metastable modification was called S_ψ .

Schenk (1956), comparing S_ψ with hexagonal selenium, proposed a preliminary unit cell containing 10 atoms placed in three turns of a cylindrical-helical mol-

ecule. These molecules would be roughly packed in a pseudo-hexagonal manner.

The cylindrical helical shape was to be expected *a priori* in view of the divalent character of the atoms, which in this kind of helix can produce the same bond angle and dihedral angle as in the well known ring molecules of the same elements (Pauling, 1949, 1960).

In a preliminary discussion and a note, by Prins & Tuinstra (1963*a, b*), it was shown that the molecule with ten atoms in three turns of the helix does not agree with the more exact measurements of the heights of the layer lines, made possible by an improvement of the X-ray diagrams. A pseudo-hexagonal indexing of the equatorial reflexions was given, and this is taken over in the present paper. On account of this indexing a structure was proposed consisting of alternating layers with left and right handed helical molecules. The indexing of the higher layer lines, proposed in this preliminary report, however, appears to need a correction.

In the present paper I give a more complete analysis of the structure of S_{ψ} , using the correct indexing and taking into account the intensities of the reflexions.

The diffraction pattern

The diffraction pattern of S_{ψ} as used by Schenk (1956) consisted of 5 layer lines with a total of 17 reflexions of measurable intensity. A certain broadening of the layer lines did not allow exact measurement of their heights. Starting from the measurements Schenk (1956) numbered the layer lines 0, 3, 4, 6, 7, and 10, the others being absent or, as in the case of number one, only indicated as a faint streak.

I improved the X-ray diagrams by heavily stretching the fibre and heating it for 40 hours at 80°C. As a result of this operation the reflexions shrank into sharp layer lines and several reflexions turned out to be doublets. The layer line numbered 1 by Schenk (1956) was now present with distinct measurable reflexions. The diffraction pattern now showed 6 layer lines with a total of about 65 reflexions.

A more exact measurement of the heights of the layer lines now made possible forces us to drop the above numbering 0, 1, 3, 4, 6, 7, and 10. For instance we obtain the value of 2.85 ± 0.03 instead of exactly 3 for the ratio of the heights of the layers '3' and '1'. In the classical conception of the fibre diagram this would force us to interpolate a large number of layer lines (with practically zero intensity) between the observed ones. As a result we have to drop the helix with ten atoms in three turns, which was only rather a good first approximation. The shortest repetition length along the fibre which can be reconciled with experiment is 78 Å. The true repetition length may be many times larger or (as I suppose) infinite.

We shall now combine this crucial point with the conception of the cylindrical helical molecule mentioned in the introduction. To obtain a sharper picture of this combination, we shall make use of the Fourier trans-

form of the helical molecule, using the elegant presentation of Cochran, Crick & Vand (1952, below referred to as C.C.V.: see also Clark & Muus, 1962).

The Fourier transform

From C.C.V. we take the transform of a helical molecule with the atoms on a cylinder. In the case of S_{ψ} , with only one kind of atom, we can for the present omit the atomic scattering factor. Moreover, all atoms are at the same distance from the axis of the cylinder. This reduces the transform to:

$$F(R, \psi, \zeta) = \sum_n J_n(2\pi Rr) \exp 2\pi i \left(n \frac{\psi}{2\pi} - n \frac{\varphi}{2\pi} + \frac{1}{2}n + \zeta z \right). \quad (1)$$

Here R , ψ and ζ are the cylinder coordinates in reciprocal space, and r , φ and z the cylinder coordinates in direct space, of the first atom of the molecule. If the next atoms are placed apart at a distance p along the axis of the molecule and P is the pitch of the helix, the sum must be taken over those values of n which satisfy:

$$\zeta = \frac{n}{P} + \frac{m}{p}, \quad (2)$$

where n and m are integers.

In the case that p/P is a rational number, (2) selects a set of regularly spaced values of ζ on which layer lines will occur. In our more general case in which p and P are incommensurable each value of ζ corresponds to a pair of integers n and m . Consequently, the transform fills the whole reciprocal space, each ζ corresponding to only one Bessel function.

The values of the Bessel function J_n with small arguments decrease rapidly as n increases. As a result, in practice, we only have to deal with terms with $|n| < 4$. In combination with this property, (2) selects a set of heights ζ corresponding to heights in the X-ray diagrams, on which observable intensities may occur. Calling the observed rows of reflexions on the films 'layer lines', it should be noted that these 'layer lines' do not correspond to one repetition length but to two: they are not classified by one integer but by two, n and m .

In order to obtain a survey of the values of ζ at which Bessel functions of low order occur we construct a three-dimensional ζ, n, m -space according to the ideas developed by Klug, Crick & Wyckoff (1958). In this space, equation (2) corresponds to a plane with the vector $(-1, 1/P, 1/p)$ as its normal. The intersection of this plane with the plane $\zeta=0$ must be drawn in such a way that the ratio of the heights of the layers '3' and '1' will be 2.85. Moreover, care must be taken that between the layer lines '1', '3' and '4' no value of ζ occurs with n integer and less than four.

In Fig. 1 the n, m -plane is drawn, the lattice points correspond to integral values of n and m . The values of ζ corresponding to the lattice points are given by (2). Since it is known that P/p will be about 3, the intersection line must be drawn more or less like the one shown

in Fig. 1. We can now visualize the correspondence between the order n of the Bessel functions and the values of ζ : Bessel functions of order 0 correspond to all lattice points with $n=0$ and consequently with the heights $\zeta=j/p$. J_1 corresponds in the same way to heights $\zeta=(b+j)/p$, J_2 to heights $\zeta=(c+j)/p$ and J_3 to heights $\zeta=(a+j)/p$, with $j=0, \pm 1, \pm 2, \pm 3, \dots$. The lowest values of ζ are the ones with $j=0$. We see at once that the heights of the first and the third layer have ratio $b:a$. The intersecting line must be drawn so as to make $b/a=2.85$. All other possibilities with $b/a=2.85$ but the one presented in Fig. 1 would result in the appearance of Bessel functions with n less than 4 and ζ between the values of layer lines 0, '1', '3' and '4'. The resulting values of P and p are 4.60 \AA and 1.37 \AA respectively.*

As we are dealing, according to our suppositions, with an incommensurable ratio of P and p it is strictly meaningless to give a layer line numbering in the classical sense of the word. The correspondence of the two numbers n and m with the observed layer lines is, how-

Table 1. Data used in the text

'Layer number'	n	m	Bessel function	$\zeta (\text{\AA}^{-1})$	$P' (\text{\AA})$
0	0	0	J_0	0	arbitrary
1	3	-1	J_3	-0.078	-38.6
2	4	-1	J_4	+0.140	+28.7
		-2	J_6	-0.156	-38.6
3	1	0	J_1	+0.217	+4.60
4	2	-1	J_2	-0.295	-6.78
5	5	-2	J_5	-0.373	-13.4
6	2	0	J_2	+0.435	+4.60
7	1	-1	J_1	-0.513	-1.95
8	6	-1	J_6	+0.574	+10.5
		-2	J_4	-0.590	-6.78
9	3	0	J_3	+0.652	+4.60
10	0	-1	J_0	-0.730	0.00

* The symbols a, b, c used here have nothing to do with the dimensions of the unit cell later on.

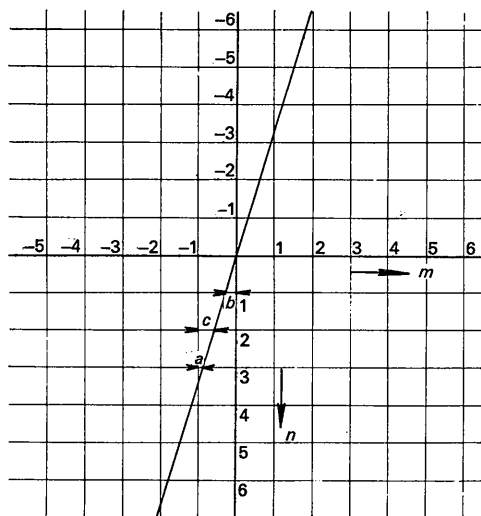


Fig. 1. Section through the ζ, n, m -space at $\zeta=0$. a, b and c are proportional to the heights of the layers 1, 3 and 4 respectively.

ever, too complicated for practical use. For this reason we prefer to use the simpler old 'effective' numbering of the layer lines. The correspondence between these 'effective' indices and the numbers n and m is shown in Table 1, where also the appropriate Bessel functions and ζ -values are given. Only Bessel functions of order less than 7 are given. On the photographs only layer lines with order of the appropriate Bessel function less than 4 occur. Since we only have to deal with one Bessel function on each layer line the square of the transform has cylindrical symmetry. In Fig. 2 the square of the Bessel function is given as a function of R , for the layer lines with $|n| < 7$. Moreover the Figure shows the two intersections of the meridional circle with the layer plane when the normal beam method is used; on the photographs only the part of the transform between these two marks may contribute to the diffracted intensity.

It should be noted that the seventh layer line intersects the meridional circle at about the maximum of the transform. At this place meridional reflexions would have a high intensity, contrary to what Liquori & Ripamonti (1959) suggest.

Effect of screw motion of the molecule

If the molecule is screwed in or out along any screw with pitch P' , the phase of (1) changes; φ and z will

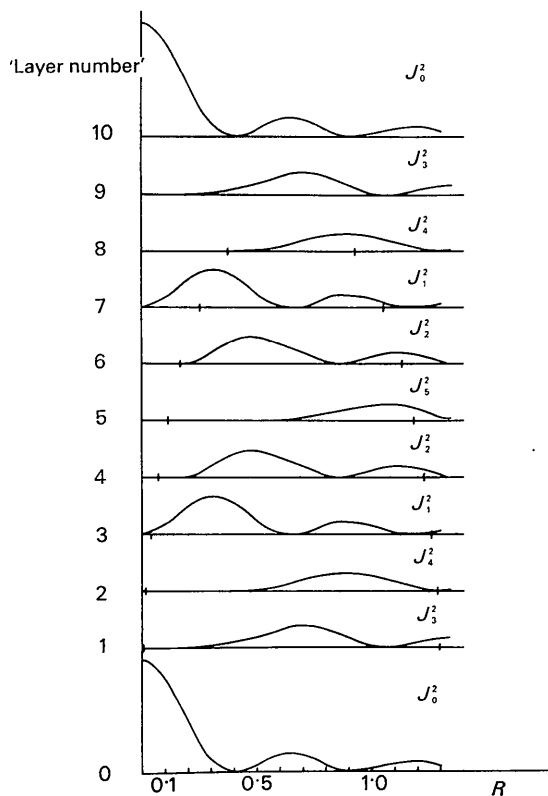


Fig. 2. Square of the 'Fourier transform' of a discontinuous helix. R is the cylinder coordinate in reciprocal space.

change, according to $\varphi/2\pi = z/P'$. Consequently for each point in reciprocal space the argument of the exponential part of (1) will be:

$$2\pi i \left[n \left(\frac{\psi}{2\pi} + \frac{1}{4} \right) - n \frac{\varphi}{2\pi} + \zeta z - z_s \left(\frac{n}{P'} - \zeta \right) \right],$$

writing z_s for the distance screwed in. When $n/P' - \zeta = 0$, the transform on the corresponding layer is unchanged after screw motion, since only one Bessel function contributes in the transform; for instance screwing in or out along the continuous basic molecular helix has not the least effect on the layer lines with $m=0$, *i.e.* on the layer lines 0, 3, 6, *etc.* To each layer line corresponds a screw motion, along a helix, that leaves the transform on the layer unchanged. In n, m -space these helices correspond to planes containing the m axis, with slope $1/P'$. Large pitches P' correspond to translations in the direction of the helical axis, very small pitches to practically pure rotations. In Table 1 the pitches P' are given for the layer lines 0 to 10. Negative pitches correspond to helices with parity opposite to the continuous basic helix. The equator appears (of course) to be insensitive to arbitrary screw motions. The first layer line will be rather insensitive to translations. Layer line 10 is insensitive to rotations. The helix leaving the layer line 4 unchanged has parity opposite to the continuous basic helix and goes either through all odd or all even atoms, counting along the molecule.

The sharpening of the first layer line in our photographs after tempering may be due to a disappearing screw disorder. The first layer line was always present with about the same, although faint, intensity. The layer lines 3 and 4 were always present with relatively sharp reflexions. From this picture it follows that layer lines 0, 3, 6, *etc.* only fix the stacking of the continuous helices, whereas for the exact positions of the atoms on these helices we have to use the information of the layers 1, 4, 7, 10 *etc.*

Besides, it should be noted, that the Bessel functions of high order not only give rise to low intensities, but that the corresponding layer lines also become diffuse after small screwing or rotational motions.

Indexing

The equatorial reflexions could be indexed with the use of a rectangular reciprocal plane lattice with sides $1/8 \cdot 11$ and $1/4 \cdot 60 \text{ \AA}^{-1}$. Because of difficulties in determining the other two angles, the higher layer lines have been indexed independently of each other, using the reciprocal plane lattice of the equatorial plane. The packing of these reciprocal layer planes to a three-dimensional lattice yielded four interesting new features:

(i) The indexing of the higher layer lines forced us to double the dimension $4 \cdot 60 \text{ \AA}$, which would suffice for the equatorial indexing, to $9 \cdot 20 \text{ \AA}$. As a consequence a^* and b^* were $1/8 \cdot 11$ and $1/9 \cdot 20 \text{ \AA}^{-1}$ respectively and the indexing formula for the equator was changed to:

$$d^{-2} = \frac{h^2}{8 \cdot 11^2} + \frac{k^2}{9 \cdot 20^2}.$$

(ii) The angle α appeared to be 90° , which in an ordinary crystallographic structure would result in a monoclinic unit cell. The axes b^* ($=b$) and a^* are perpendicular to the fibre direction.

(iii) The doubling of the dimension b to $9 \cdot 20 \text{ \AA}$ gave rise to a systematic extinction rule not only for the equator but also for the higher layers. This peculiar systematic extinction rule is shown in Fig. 4.

(iv) It was impossible to find an angle β within reasonable limits. The smallest angle β which could be reconciled with the measured reflexion positions was in the neighbourhood of 170° . This suggests again a very large repetition length in the fibre direction. For in that

Table 2. Intensities and indexing of reflexions

Q_0	Q_c	I_0	I_c	hkl	Q_0	Q_c	I_0	I_c	hkl	Q_0	Q_c	I_0	I_c	hkl	Q_0	Q_c	I_0	I_c	hkl						
152	-	0	100	-	2751	-	0	531	1165	1170	-	1051	-	45	414	-	6456	-	1	766					
473	472	s	120	020	2978	2953	m	38	411	1222	1222	s	200	203	4093	4064	m	38	514	-	6508	-	1	266	
613	624	vs	400	200	-	3022	-	34	051	1414	1425	s	235	223	-	4154	-	24	454	-	6584	-	7	606	
-	1080	-	3	220	3255	3231	m	23	451	1691	1694	w	42	223	4751	4761	w	4	254	-	6779	-	5	246	
-	1368	-	0	300	3258	3258	m	11	351	-	2049	-	0	303	-	4768	-	18	354	-	6864	-	6	426	
1842	1840	w	5	320	3470	3464	m	26	251	2104	2118	m	68	325	-	1918	-	-	006	2732	2738	vs	160	017	
2050	2042	vw	3	040	3560	3571	m	53	511	-	2369	-	92	143	-	1935	-	-	106	2808	2804	vs	182	117	
2431	2432	s	22	400	3860	3898	w	55	351	2500	2521	s	85	323	-	2204	-	0	306	2950	2976	vw	19	117	
2470	2498	m	13	240	-	4141	-	2	351	-	2588	-	38	145	2250	2256	m	17	206	-	3174	-	7	217	
2868	2904	vw	2	420	-	4405	-	1	511	-	2643	-	38	403	2379	2390	s	17	026	3470	3518	m	116	217	
3244	3258	w	8	340	-	4516	-	5	511	-	2843	-	0	245	-	2407	-	35	126	3712	3683	s	13	037	
-	3800	-	0	500	-	4641	-	5	351	-	3112	-	25	243	2579	2590	s	1	356	3749	3749	m	80	337	
4265	4252	s	7	060	5130	5121	w	28	451	3110	5115	m	11	423	2707	2728	m	52	226	3867	3848	vs	108	317	
-	4272	s	30	520	-	5160	-	6	611	3517	3536	w	16	345	2800	2795	m	31	206	3867	3921	vs	112	37	
4316	4322	m	25	440	-	5350	-	9	351	-	1016	-	0	014	-	2882	-	0	306	4136	4119	m	65	337	
4845	4860	w	11	260	5900	5788	w	26	071	-	1018	-	1	114	2884	3267	m	60	226	4337	4364	w	26	317	
5449	5472	w	10	600	-	5926	-	1	171	1318	1319	vw	1	214	-	3354	-	1	326	-	4463	-	6	237	
5618	5620	w	10	360	-	6093	-	3	171	1318	1423	vw	1	214	-	3690	-	0	306	4337	4364	w	26	317	
-	5944	-	1	620	6200	6105	w	24	631	-	1926	-	92	214	3797	3812	s	38	046	4136	4119	m	65	337	
-	187	-	0	011	-	6293	-	8	271	-	1933	-	87	314	-	3825	-	3	146	5414	5417	m	298	0	1
-	256	-	0	111	-	6406	-	10	551	1942	1963	vs	46	034	4094	4094	s	60	146	5414	5550	m	226	1	10
-	423	-	0	111	-	6532	-	6	271	2250	2264	w	2	134	4172	4162	s	38	326	5552	5567	m	188	1	10
-	629	-	2	211	-	6976	-	13	371	-	2268	-	15	234	4172	4162	s	38	326	6017	5987	vw	25	2	10
962	962	vw	20	211	-	7053	-	11	371	-	2837	-	1	314	4284	4284	s	50	426	6017	5987	vw	22	2	10
1146	1132	vw	18	031	-	7106	-	9	851	2866	2816	m	16	414	-	4685	-	1	246	-	4772	-	21	346	
-	1201	-	5	131	-	7240	-	10	351	-	2876	-	84	234	-	4889	-	20	306	-	5045	-	0	506	
1300	1306	m	35	311	-	7476	-	10	371	-	2878	-	13	334	-	5045	-	0	506	-	5361	-	7	426	
1361	1368	m	35	331	-	7476	-	10	371	-	2878	-	13	334	-	5361	-	7	426	-	5361	-	7	426	
-	1574	-	2	151	-	7476	-	10	371	3792	3791	m	24	334	-	5517	-	9	526	-	5517	-	9	526	
-	1806	-	1	311	-	7476	-	10	371	-	3792	-	48	054	4172	4162	s	38	326	5980	5980	vw	24	346	
1933	1907	vw	25	231	946	951	vs	420	023	-	3853	-	0	354	-	5702	-	6	446	-	6170	-	13	046	
2250	2251	w	31	331	-	953	-	260	203	-	3853	-	0	354	-	6170	-	13	046	-	6187	-	14	166	
-	2286	-	2	411	-	1036	-	12	123	-	3853	-	0	354	-	6392	-	0	506	-	6392	-	0	506	

case the true first layer would be very close to the equatorial one, which causes the c^* axis to be turned over a very large angle around the b^* axis before it can be made to coincide with a reciprocal lattice row again.

We propose now that the repetition length along the fibre be taken as infinite and the angle β as undetermined.

It will be clear now that only in the direction of the b^* axis is an ordinary indexing possible. For the index l we will use the layer number as tabulated in Table 1. For the origin of the h index in each reciprocal lattice layer we will use the point nearest to the origin in reciprocal space. This 'indexing' is shown in Table 2; the Q values used in this table correspond to $10^4/d^2$ (d in Å).

The unit cell

The repetition length along the helical molecules being infinite causes the 'unit cell' to contain an infinite number of atoms. This kind of 'unit cell' is neither usual

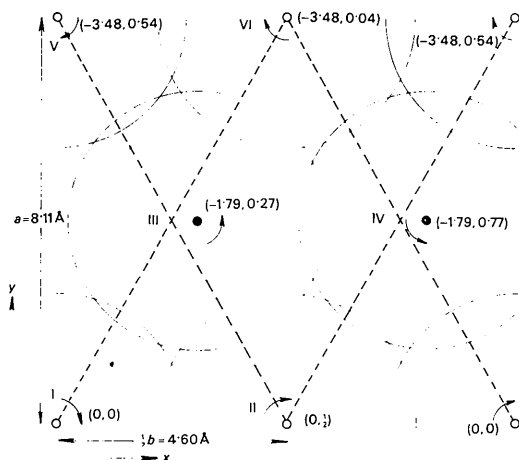


Fig. 3. Projection of the structure of S_ψ along the axes of the helical molecules. ○ right handed molecules, ● left handed molecules. The numbers in brackets ($z_t, z_s/p$) mean a translation z_t of the continuous molecular helix along its axis, in combination with a screw motion of the molecule along the continuous helix over a fraction z_s/p of the atomic distance.

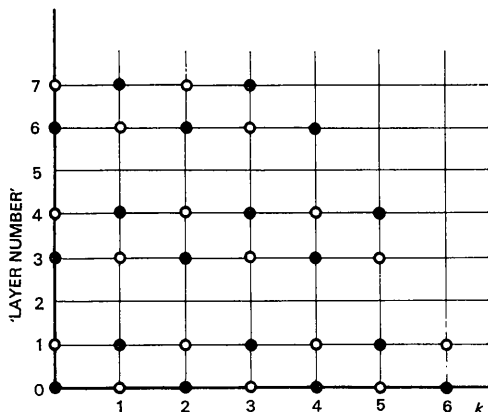


Fig. 4. The systematic extinction rule. Extinction occurs for (○). On the other reciprocal lattice rows (●) reflexions occur.

nor useful in the analysis of the structure. We can, however, construct a pseudo-rhombic 'partial' unit cell with dimensions $a=8.11$, $b=9.20$, and $c=1.37$ Å, using for the third dimension of the unit cell the parameter p , the atomic distance along the axis of the molecular helix, a and b being perpendicular to this axis. Using the density of 1.9 for S_ψ given by Schenk (1956), this pseudo unit cell contains four sulphur atoms. Combination of this fact with the conception of the helical molecules leads to a two-dimensional packing of the infinite helical molecules in such a way that the area $a \times b$ contains the projections, along their axis, of four helices. All atoms of the four infinite helical molecules will be projected in this way on four equal circles in the area $a \times b$.

Table 2 and Fig. 4 show the absence of the reflexions in the equatorial plane with k odd. Combination of this fact with the absence of the $h00$ reflexions with h odd, while the even reflexions on the k axis are present, results in an arrangement of the projections of the molecules in the area $a \times b$ shown in Fig. 3: in a layer of molecules in the b direction the molecules are shifted from the centred positions.

Coordinates

The molecules are completely determined by:

- (i) Their handedness or parity,
- (ii) The radius of the helical cylinder, r ,
- (iii) The pitch of the helix, P ,
- (iv) The atomic distance along the cylinder axis, p .

We already know the last two. In the next paragraph we shall determine the parity; the radius will be determined in the last section.

The position and orientation of the molecules in the structure are determined by:

- (i) The orientation of the helical axis, being normal to the a, b -plane.

(ii) The positions of this axis in the area $a \times b$. This position is determined by the coordinates x and y , which are fractional coordinates in the b and a directions respectively. The conjugated coordinates in reciprocal space being $\xi = Rb \cos \psi$ and $\eta = Ra \sin \psi$ respectively. Note that in this way b and k correspond to ξ while a and h correspond to η . This is due to C.C.V. using right handed coordinates and a, b and c forming a left handed set.

(iii) The orientation of the continuous helix around the helical axis, determined by z_t , the distance from the point on the continuous helix with $\varphi=0$, to the reference plane $z=0$.

(iv) The above parameters being constant there remains only one degree of freedom for the molecule, *viz.* translation of the atoms along the continuous helix, the atoms remaining equidistant; we call this screwing in or out. The corresponding parameter is z_s , being the distance in the z direction from the point with $\varphi=0$ to the nearest atom. This atom was called the *first* atom of the molecule. The total z coordinate is $z_t + z_s$.

It should be noted that a translation of the molecule as a whole, of the two z coordinates, only affects z_t , while a screw motion of the molecule along the basic continuous helix only affects z_s .

The packing of the molecules

In the arrangement of the molecular axes, as shown in Fig. 3, the distances between the molecular axes are not equal. This points to the occurrence of left and right handed screws. As our policy is to use Fourier transforms, we must distinguish now between the transform of a left handed and that of a right handed molecule.

A continuous helix is defined by:

$$x = r \cos 2\pi z/P; \quad y = r \sin 2\pi z/P; \quad z = z.$$

By the sign of the pitch a difference can be made between left and right handed screws, the right handed screws having positive pitch P_r and the left handed ones having negative pitch P_l . From (2) it follows that for the left handed screw n_l is negative at the same value of ζ . Thus: $P_l = -P_r$ and $n_l = -n_r$, $m_l = m_r$ and $p_l = p_r$ and consequently

$$J_{n_l}(x) = (-1)^{n_r} J_{n_r}(x).$$

If the molecule is translated with translation components $(x, y, 0)$, the transform must be multiplied by $\exp 2\pi i(x\xi + y\eta)$. The arguments of the Fourier transforms for the right and left handed molecules are now, if we use (1) and write n for n_r :

$$n \frac{\psi}{2\pi} - n \frac{\varphi}{2\pi} + \frac{1}{4}n + x\xi + y\eta + z\zeta$$

and

$$-n \frac{\psi}{2\pi} + n \frac{\varphi}{2\pi} + \frac{1}{4}n + x\xi + y\eta + z\zeta$$

respectively.

Separating z into z_t and z_s the part z_s is related to φ by:

$$\varphi/2\pi = z_s/P,$$

P being $\pm P_r$. With the use of (2) the φ can be eliminated:

$$\mp n \frac{\varphi}{2\pi} + z_s\zeta = z_s \left(-\frac{n}{P} + \zeta \right) = m \frac{z_s}{p}.$$

The transforms now reduce to:

(i) For the right handed screw:

$$J_n(2\pi Rr) \exp 2\pi i \left[n \frac{\psi}{2\pi} + \frac{1}{4}n + \frac{mz_s}{p} + x\xi + y\eta + z_t\zeta \right].$$

(ii) For the left handed screw:

$$J_n(2\pi Rr) \exp 2\pi i \left[-n \frac{\psi}{2\pi} + \frac{1}{4}n + \frac{mz_s}{p} + x\xi + y\eta + z_t\zeta \right].$$

If we accept, for the present, the occurrence of left and right handed molecules it is reasonable that two of the four molecules in the 'unit cell' are of the left handed and the other two of the right handed type. There are now two possibilities; either each layer of molecules in the \mathbf{b} direction contains only specimens with the same parity, or each layer contains alternating molecules of opposite parity.

In the \mathbf{b} direction the distances between the molecular axes are all equal. So the operation, bringing a molecule in coincidence with its neighbour, will be the same for all molecules. The repetition length in the \mathbf{b} direction is twice the molecular distance, so the operation applied twice to a molecule must bring it in exactly the original orientation. The only possible operations doing this are: (i) change of the parity, (ii) screwing in or out over $\frac{1}{2}p$, (iii) doing nothing; all three combined with the translation $(\frac{1}{2}b, 0, 0)$.

As will be shown now, with the aid of the Fourier transform of the 'unit cell', operation (ii) (screwing in or out over $\frac{1}{2}p$) generates exactly the peculiar systematic extinction rule of Fig. 4. In order to show this we will take together the four molecular transforms with the following coordinates:

$$\begin{aligned} \text{Molecule I: } & x^I = 0, y^I = 0, z_s^I = 0, \\ & z_t^I = 0, \text{ right handed,} \\ \text{Molecule II: } & x^{II} = \frac{1}{2}, y^{II} = 0, z_s^{II} = \frac{1}{2}p, \\ & z_t^{II} = 0, \text{ right handed,} \\ \text{Molecule III: } & x^{III} = x, y^{III} = \frac{1}{2}, z_s^{III} = z_s, \\ & z_t^{III} = z_t, \text{ left handed,} \\ \text{Molecule IV: } & x^{IV} = x + \frac{1}{2}, y^{IV} = \frac{1}{2}, z_s^{IV} = z_s + \frac{1}{2}p, \\ & z_t^{IV} = z_t, \text{ left handed.} \end{aligned}$$

Adding these transforms we obtain the transform of the 'unit cell':

$$\left[J_n(2\pi Rr) \exp 2\pi i \left(\frac{n\psi}{2\pi} + \frac{1}{4}n \right) \right] \times [1 + \exp 2\pi i(\frac{1}{2}m + \frac{1}{2}\zeta)] \times [1 + \exp 2\pi i\chi],$$

where

$$\chi = \left(-n \frac{\psi}{\pi} + x\xi + \frac{1}{2}\eta + z_t\zeta + m \frac{z_s}{p} \right).$$

The transform consists of the transform of molecule I multiplied by two fringe factors.

The first fringe factor is zero for $m + \zeta = \text{odd}$; so, using Table 1, extinction occurs for:

m	layer numbers	k
0	0, 3, 6, 9, ...	odd
1	1, 2, 4, (8), 11, ...	even
2	(2), 5, 8, ...	odd

etc.

At all other values of k the first fringe factor will be 2 exactly. These extinctions correspond exactly to the observed ones, for $m=0$ and $|m|=1$; the layer lines with $|m| > 1$ are not observed because of the high order of the appropriate Bessel functions or because of ζ being very high.

If we had taken the other possibility, the molecules in the \mathbf{b} direction having alternating opposite parity,

a term with ψ would have entered the argument of the first fringe factor, with the result that the calculated extinctions would no longer correspond to the observed ones.

Moreover, if we chose for the molecules III and IV the same parity as for molecules I and II the term with ψ would disappear in the argument of the second fringe factor. This would cause alternating presence and absence of the reflexions along reciprocal lattice rows with l and k constant. This conflicts with the observations. So the structure consists of layers of molecules in the direction of the b axis. The molecules in such a layer all have the same parity, and are screwed in or out over half the atomic period, with respect to each other. Molecules of neighbouring layers have opposite parity.

In the second fringe factor the unknown parameters are x , z_t and z_s , while the first factor of the transform contains the unknown parameter r . The parameters z_t can be determined, with the use of the information of layer lines 0, 3, 6, *etc.* alone, in the following way. Of the two parameters z_t and z_s , only z_t has to deal with the packing of the continuous helices; the term with z_s is missing in the argument of the transforms of layer lines 0, 3, 6, *etc.*, m being zero. Taking into account these layer lines only, an analysis would result in a structure consisting of continuous helices. This structure would be monoclinic with space group $P2$. The unit cell would contain parts of only two con-

tinuous helices of opposite parity, these parts being only one complete turn of the screw. The unit-cell dimensions would be: $a=8.86 \text{ \AA}$ ($=8.11 \sin \beta$), $b=4.60 \text{ \AA}$ ($=9.20/2 \text{ \AA}$) and $c=4.60 \text{ \AA}$ ($=P$), $\alpha=\gamma=90^\circ$, $\beta=114^\circ$. The twofold axis is parallel to the b axis and going through a point of the helix having zero a coordinate. From such a partial analysis the parameter z_t can be determined taking in account the intensities of the reflexions; z_t appeared to be -1.79 \AA . This value of z_t is equal to $(8.11/2) \cot \beta$; this shows, after some geometrical considerations, that when the helical line of helix II (see Fig. 3) is nearest to the axis of helix III, the helical line of III must be at the opposite side of its helical axis. This means that the helices II, III and IV are packed with maximal 'interlocking'. Screws with opposite parity always fit better than screws with the same parity.

In an analogous way one can consider the layer lines 0, 10, 20, *etc.*, corresponding to the repetition length p only. This would result in a monoclinic centred structure, consisting of atoms placed apart at a distance p on the axes of the helices considered above.

Layer lines not belonging to the two series discussed above are due to the occurrence of both repetition lengths p and P , as 'intercombinations'; they correspond to 'off-axis' lattice points in Fig. 1.

Returning now to the analysis of the real structure of the discontinuous helices, taking into account the intensities of all observed reflexions, we can again

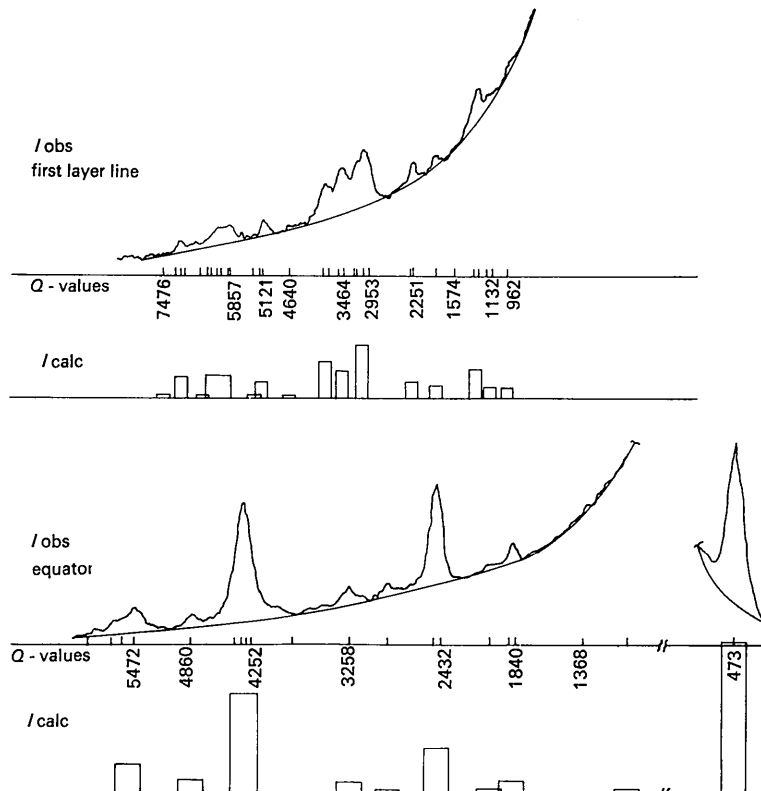


Fig. 5. Comparison of observed and calculated intensities on layer lines 0 and 1 respectively.

check the value of z_t (which proved to be correct) and determine the values of the remaining unknown parameters. For quite a number of values of the parameters x , r and z_s the intensities have been calculated. The best agreement with the observed ones occurred for $r=0.96 \text{ \AA}$, $z_s/p=0.27$ and $x=0.29$. The intensities appeared to be quite insensitive to variations in x .

Summarizing, the structure of S_w consists of long helical molecules, with an infinite repetition length along the helix, all having the same orientation of the helical axis. This orientation is called the c axis of the structure. The molecules are arranged in flat layers each containing only molecules of equal parity. The direction in such a molecular layer and normal to the helical axis is called the b direction. A layer of molecules is placed beside its neighbour in the following way: The parity is inverted; the helical axes are shifted in the b direction over $0.29 \times 9.20 = 2.67 \text{ \AA}$, that is about 0.4 \AA from the centered positions, as shown in Fig. 3; the continuous helices are shifted in the c direction over -1.79 \AA , while the molecules are screwed upwards over $0.27 \times 1.37 = 0.37 \text{ \AA}$. As a result no monoclinic angle could be determined and for this reason we chose for the 'a direction' the direction normal to the plane of the b - and c axes.

The S_w molecule

One of the parameters determined above is the radius of the helical cylinder, 0.96 \AA . Going from one atom to the next one on the same molecule this radius has to be turned through $107^\circ 27' \pm 40'$ and shifted along the cylinder axis over $1.373 \pm 0.005 \text{ \AA}$. From these values we obtain the bond distance as $2.069 \pm 0.014 \text{ \AA}$, the bond angle $106.0^\circ \pm 1.7^\circ$ and the dihedral angle $84.2 \pm 1.0^\circ$. In Table 3 these quantities are compared with those of other sulphur molecules S_6 and S_8 (see for instance Donohue, Caron & Goldish, 1961), and an S_{12}^* . The errors given in Table 3 are standard deviations.

Table 3. *Molecular dimensions*

Molecule	Bond distance	Bond angle	Dihedral angle
S_6 (in S_8)	$2.057 \pm 0.018 \text{ \AA}$	$102.2 \pm 1.6^\circ$	$74.5 \pm 2.5^\circ$
S_8 (in S_8)	2.059 ± 0.002	107.9 ± 0.6	98.9 ± 0.7
S_∞ (in S_w)	2.069 ± 0.014	106.0 ± 1.7	84.2 ± 1.0
S_{12}^*	—	107.5 ± 2.5	87.2 ± 1.5

Experimental details

With the aid of the normal beam method the reflexions on the layer lines 0, 1, 3, 4, 6, and 7 have been observed, while for the reflexions on the tenth layer line and some nearly diatropic reflexions on the layer lines 6 and 7

* It is possible to construct S_{12} rings, in a way overlooked by Pauling (1949), as follows: Six atoms form a regular hexagon; the other six are placed in two equilateral triangles in planes equidistant above and below the hexagonal plane. The molecule would have symmetry $\bar{3}$ (S_6 in the Schoenflies notation).

the inclined beam method has been used. On the layer lines 7 and 10 intensities have been estimated visually. The photometer recordings of the other layer lines are given in Figs. 5 and 6.

In Table 2 and in the photometer recordings the calculated intensities I_{calc} are compared with the observed ones. The calculated intensities have not been corrected for thermal vibration, which could not be determined correctly. The calculation is carried out with the aid of graphical methods and as a result the I_{calc} may be in error by about 5%. In the scale (Figs. 5 and 6) the areas of the plotted rectangles correspond to the calculated intensities (Table 2), the scale factor for each layer line being an arbitrary one. This was done because of the lack of information for calculating the temperature and scale factors. The Q values are $10^4/d^2$ (d in \AA); the marks on the scale correspond to reciprocal lattice points shown in Table 2. The photometer recordings have been determined only in the direction of the layer line. I_{calc} has been corrected so as to compare directly with the observed intensities in

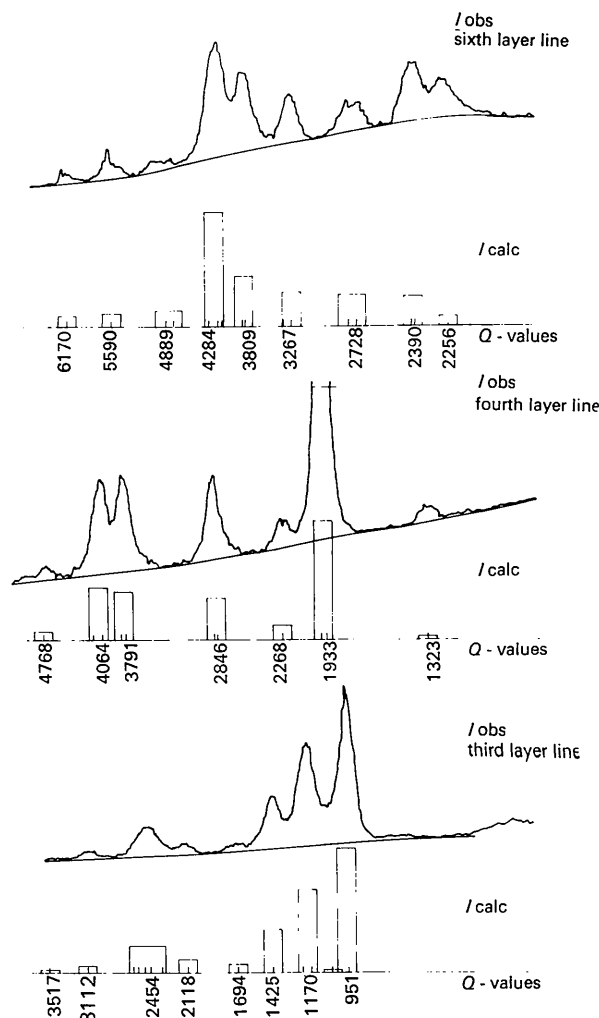


Fig. 6. Comparison of observed and calculated intensities on layer lines 3, 4 and 6.

the photometer recordings. On the equator the reflexion with $Q=613$, *vs*, has been omitted because of its very high intensity, being about ten times that with $Q=473$. For the 6th layer line the nearly meridional reflexions are smeared out along the layer line, which fact may be responsible for the high intensities observed. There is a good agreement between the observed and calculated intensities.

The author wishes to thank Dr J. H. Palm for critical discussions and Professor Dr J. A. Prins for stimulating guidance.

References

- CLARK, E. S. & MUUS, L. T. (1962). *Z. Kristallogr.* **117**, 108.
 COCHRAN, W., CRICK, F. H. C. & VAND, V. (1952). *Acta Cryst.* **5**, 581.
 DE HAAN, Y. M. (1958). *Physica*, **24**, 855.
 DONOHUE, J., CARON, A. & GOLDISH, E. (1961). *J. Amer. Chem. Soc.* **83**, 3748.
 KLUG, A., CRICK, F. H. C. & WYCKOFF, H. W. (1958). *Acta Cryst.* **11**, 199.
 LIQUORI, A. M. & RIPAMONTI, A. (1959). *Ric. Sci.* **29**, 2186.
 MEYER, K. H. & GO, Y. (1934). *Helv. Chim. Acta*, **17**, 1081.
 PAULING, L. (1949). *Proc. Nat. Acad. Sci. Wash.* **35**, 495.
 PAULING, L. (1960). *The Nature of the Chemical Bond*, p. 135. Ithaca: Cornell Univ. Press.
 PRINS, J. A., SCHENK, J. & HOSPEL, P. A. M. (1956). *Physica*, **22**, 770.
 PRINS, J. A., SCHENK, J. & WACTERS, L. H. J. (1957). *Physica*, **23**, 746.
 PRINS, J. A. & TUINSTR, F. (1963a). *Physica*, **29**, 328.
 PRINS, J. A. & TUINSTR, F. (1963b). *Physica*, **29**, 884.
 SCHENK, J. (1956). *Enige Onderzoekingen in Verband met de Moleculaire Bouw van Amorfe Zwavel*. Thesis, Delft.
 TRILLAT, J. J. & FORESTIER, H. (1932). *Bull. Soc. Chim. Fr.* **51**, 248.

Acta Cryst. (1966). **20**, 349

Refinement of the Structure of Bisthiourea-nickel (II) Thiocyanate.

BY M. NARDELLI, G. FAVA GASPARRI, G. GIRALDI BATTISTINI AND P. DOMIANO

Structural Chemistry Laboratory, Institute of Chemistry, University of Parma, Italy

(Received 15 June 1965)

The crystal structure of $\text{Ni}[\text{SC}(\text{NH}_2)_2]_2(\text{NCS})_2$ has been refined by means of three-dimensional differential syntheses. Each nickel atom lies on a symmetry centre (space group $P\bar{1}$) and is octahedrally surrounded by four sulphur atoms from thiourea molecules ($\text{Ni-S } 2.53 \pm 0.01$ and 2.56 ± 0.01 Å) and two nitrogen atoms from thiocyanate groups ($\text{Ni-N } 1.99 \pm 0.01$ Å). The octahedra are linked in chains with each thionilic S atom shared by two adjacent nickel atoms. Bond distances and angles are discussed.

The structure of bisthiourea-nickel(II) thiocyanate, $\text{Ni}[\text{SC}(\text{NH}_2)_2]_2(\text{NCS})_2$, was determined several years ago by Nardelli, Braibanti & Fava (1957) (hereafter called NBF) by means of generalized Fourier syntheses using an incomplete set of three-dimensional data (482 independent reflexions out of 1222 possible with $\text{Cu } K\alpha$ radiation). Because this compound is interesting from the point of view of the coordination of the thionilic sulphur and the thiocyanate group, the refinement of its structure was undertaken to improve the reliability of bond distances and angles with the use of all the observable data with $\text{Cu } K\alpha$ radiation.

Cell constants, remeasured, from rotation and Weissenberg photographs, are as follows:

$\text{Ni}[\text{SC}(\text{NH}_2)_2]_2(\text{NCS})_2$. $M = 327.1$; $a = 3.80 \pm 0.01$, $b = 7.58 \pm 0.01$, $c = 10.11 \pm 0.01$ Å; $\alpha = 92.3 \pm 0.2$, $\beta = 98.1 \pm 0.2$, $\gamma = 104.1 \pm 0.1^\circ$, $V = 278.7$ Å³, $Z = 1$, $D_x = 1.95$, $D_m = 1.88$ g.cm⁻³ (flotation), $\mu = 90.2$ cm⁻¹ ($\text{Cu } K\alpha$). Space group: $P\bar{1}$.

New three-dimensional intensity data were collected from integrated and non-integrated multiple film

Weissenberg photographs taken around [100] with a sample of nearly square cross-section (edge 0.008 cm) and around [010] using a fragment with a mean radius of 0.008 cm. All the crystals were parallel twins with twinning axis [100], and yet the reflexions due to the two individuals were well separated in all the photographs (excepting of course the $0kl$ reflexions which were always superimposed). The complete indexing and intensity measurement (photometrically) of the spots from both individuals were straightforward in the series of photographs taken around [100]. In the series taken around [010], only the reflexions due to the individual rotating around that axis were considered. Four levels about the a axis and seven levels about the b axis were measured, giving a total of 1010 observed independent reflexions. The absorption correction for cylindrical samples was applied to [100] – and for spherical samples to [010] – data. Upper-level Weissenberg spot shape effects were considered following Phillips (1956) for the first series and following Scouloudi (1953) for the second series of data. The structure amplitudes (with the exception of $0kl$) were put on the same relative scale by the least-squares cross-correl-